Navigation Performance Comparison of ACE-BOC Signal and TD-AltBOC Signal

Chunxia Li, Jianjun Fan(✉), Min Li, and Yang Gao

Beijing Satellite Navigation Center, Beijing 100094, China
xiaomangps@163.com

Abstract. With the development of intellectual property rights and navigation performance optimization, recently two new four-components signal multiplex modulation methods, ACE-BOC & TD-AltBOC have been brought forward by scholars. The navigation performances of them are aimed to be compared in this paper. Based on analyzing of the power spectrum density function of these two modulation methods, their main navigation performances of code tracking precision, anti-multipath capability, anti-jamming capability and compatibility are compared. The results show that the navigation performance of ACE-BOC modulation signal is 1.0 dB–2.1 dB prior to that of the TD-AltBOC modulation signal. This is because of the difference of their power spectrum density function figures and that of the 1.2 dB distributed power level. The study production can be referred to choose the better one between these two new modulation methods.

Keywords: ACEBOC · TD-AltBOC · Multiplex · Modulation · Performance

1 Introduction

Both the GPS L5 signal and the Galileo E5 signal are used to design the signal of civil aviation service signal or life safety service. Considering the demand of high integrity of civil aviation, the satellite navigation signal design of each satellite navigation system in this frequency band tends to interoperate with GPS L5 and Galileo E5 signals. Beidou global satellite navigation system B2 frequency point civil signal design also adhering to this idea, trying to get as close as possible to Galileo AltBOC modulation signal. However, limited by Galileo AltBOC modulation of intellectual property rights, China has to seek a new four signals constant-envelope multiplex modulation technique [1–3]. Under this background, in recent years, two scholars from Huazhong University of Science and Technology and Tsinghua University have proposed two modulation modes: TD-AltBOC [4–6] and ACE-BOC [7–13].

At present, the public papers on the systematic comparative study of the two modulation modes are rare. This paper attempts to compare the performance differences between the two modulation modes and analyze the underlying causes behind them. Considering that the method based on receiver test is limited by the implementation method and parameters of the receiver, this paper uses the theoretical performance analysis method to compare the performance of the two modulation modes. At the same time, because the time domain analysis is related to the specific pseudo-code sequence design, this paper attempts to analyze the causes of the performance

S. Han et al. (Eds.): AICON 2019, LNICST 287, pp. 52–64, 2019.
https://doi.org/10.1007/978-3-030-22971-9_5

difference between the two modulation modes from the angle of power level and power spectral density by using the frequency domain analysis method.

Firstly, the definition and power spectrum of TD-AltBOC modulation signal and ACE-BOC modulation signal are studied, and then the pseudo-code tracking precision, anti-multipath ability, anti-jamming ability and compatibility of these two modulation signals are compared and analyzed. In terms of anti-jamming ability, DME/TACAN pulse interference is the actual interference faced by L5/E5/B2 frequency point signal reception, however, the method of pulse hiding can effectively combat it, so the following two common interference types of matching spectrum interference and single carrier interference are analyzed in this paper. In terms of compatibility, pseudo-code sequence cross-correlation characteristics and spectral separation coefficients are two common analytical methods, the former method is closely related to the specific pseudo-code sequence design, so this paper adopts the latter method.

2 ACE-BOC Modulated Signal and TD-AltBOC Modulated Signal

2.1 ACE-BOC Modulated Signal Definition and Spectrum

ACE-BOC Signal Definition. Asymmetric constant Envelope BOC (Asymmetric Constant Envelop BOC ACE-BOC Multiplexing) is a new dual-frequency multiplexing modulation technique proposed by Tsinghua University, which can modulate four independent spread spectrum codes in two different carrier frequencies with arbitrary power ratio combinations.

Note four different bipolar baseband spread spectrum signals as $S_{\mathrm{UI}}(t)$, $S_{\mathrm{UQ}}(t)$, $S_{\mathrm{LI}}(t)$, $S_{\mathrm{LQ}}(t)$. To combine these four baseband signals to a composite signal with constant envelope with splitting spectrum, where $S_{\mathrm{UI}}(t)$, $S_{\mathrm{UQ}}(t)$ modulated on the upper side with the same phase, orthogonal components, respectively, and $S_{\mathrm{LI}}(t)$, $S_{\mathrm{LQ}}(t)$ modulated on the lower side with the same phase, orthogonal components, respectively, then the optimal solution is ACE-BOC modulation. If the frequency interval of the upper sideband and lower sideband is $2f_s$, and the central frequency is f_ω, then radiofrequency ACE-BOC modulation can be expressed as

$$S_{\mathrm{ACE,RF}}(t) = \mathrm{Re}\{S_{\mathrm{ACE}}(t)\exp(j\pi 2f_\omega t)\} \tag{1}$$

Where $S_{\mathrm{ACE}}(t)$ is complex baseband ACE-BOC signal, which can be expressed as:

$$S_{\mathrm{ACE}}(t) = \frac{\sqrt{2}}{2}\alpha_{\mathrm{I}}\,\mathrm{sgn}[\sin(2\pi f_s t + \varphi_{\mathrm{I}})] + j\frac{\sqrt{2}}{2}\alpha_{\mathrm{Q}}\,\mathrm{sgn}\left[\sin(2\pi f_s t + \varphi_{\mathrm{Q}})\right] \tag{2}$$

In this equation, the additional phase of real number and imaginary parts is

$$\begin{cases} \phi_{\mathrm{I}} = -\operatorname{atan} 2(S_{\mathrm{UI}} + S_{\mathrm{LI}},\, S_{\mathrm{UQ}} - S_{\mathrm{LQ}}) \\ \phi_{\mathrm{Q}} = \operatorname{atan} 2(S_{\mathrm{UQ}} + S_{\mathrm{LQ}},\, S_{\mathrm{UI}} - S_{\mathrm{LI}}) \end{cases} \tag{3}$$

Where $\operatorname{atan} 2(\cdot,\cdot)$ is anti-tangent function.

The four components of the ACE-BOC modulated signal can be combined with arbitrary power ratio, in which the symmetric four-component combination of unequal power is the most feasible. In this power distribution, the same phase and orthogonal components of each edge band have different power, but the total power of the upper and lower side bands is the same, which is

$$P_{\mathrm{UQ}} : P_{\mathrm{LQ}} : P_{\mathrm{UI}} : P_{\mathrm{LI}} = 1 : 1 : \beta^2 : \beta^2 \tag{4}$$

Where P_{UQ}, P_{LQ}, P_{UI}, P_{LI} is the power of the signal $S_{\mathrm{UQ}}(t)$, $S_{\mathrm{LQ}}(t)$, $S_{\mathrm{UI}}(t)$, $S_{\mathrm{LI}}(t)$ respectively. Without losing its general, suppose $\beta^2 \geq 1$. This type of ACE-BOC signal can provide different power ratios for each side band's data channel and pilot channel. In order to optimize the robustness and measurement accuracy of tracking, it is often hoped that the pilot channel will have higher power. In this paper, the ACE-BOC modulation signal is studied in the following focus, and when the specific sub-carrier frequency and pseudo-code frequency are introduced, the modulation mode can be expressed as ACE-BOC($f_s, R_c; [1, 1, \beta^2, \beta^2]$) or simplified as $\mathrm{ACE} - BOC(m, n, \beta^2)$, where $m = f_s/(1.023 \times 10^6\,\mathrm{MHz})$ and $n = R_c/(1.023 \times 10^6\,\mathrm{MHz})$, R_c represents pseudo-random code rate.

As mentioned above, the advantage of ACE-BOC modulated signal is that on the basis of AltBOC modulated signal, the power ratio between the data channel and the pilot channel is adjusted to obtain better signal performance.

ACE-BOC Signal Spectrum. The spectrum of ACE-BOC modulated signal $G_{\mathrm{ACE-BOC}}(f)$ is [14]

$$G_{\mathrm{ACE-BOC}}(f) = \frac{R_c \cos^2\left(\frac{\pi f}{R_c}\right)\left\{1 - \cos(6\varphi)[\sin(5\varphi)\sin\varphi + \cos^2\varphi]\right\}}{2\pi^2 f^2 \cos^2(6\varphi)} \tag{5}$$

Where $\varphi = \frac{\pi f}{12 f_s}$.

2.2 TD-AltBOC Modulated Signal Definition and Spectrum

TD-AltBOC Signal Definition. The Galileo system uses quadrupole carrier AltBOC modulation at the E5 frequency, and its baseband waveform flip rate is 8 times the subcarrier frequency, and the product is attached to maintain the constant envelope [15]. When four different PN codes are used, there is no doubt that this modulation greatly increases the complexity of the receiver. Time-division multiplexing is another modulation method that joint the constant envelope of four E5 signal components, which uses a code-by-bit multiplexing method, and emits only 2 signal components at any moment, so that the constant envelope can be obtained without the addition of the product item [4]. This modulation method is called time-division AltBOC, which is recorded as TD-AltBOC. When the specific sub-carrier frequency and pseudocode frequency are introduced, the modulation mode can be abbreviated as $\mathrm{TD} - AltBOC(m, n)$.

Using TD-AltBOC modulation, the subcarrier is bipolar, and the baseband waveform flip rate is only 4 times the subcarrier frequency. Its signal generation and reception complexity is similar to BOC modulation. In addition, the reuse efficiency is 100%, which makes it feasible to use larger emission and receive bandwidth containing harmonics for further performance improvements.

As mentioned above, the advantage of the TD-AltBOC signal is that the implementation complexity is lower than that of the AltBOC modulation signal.

TD-AltBOC Signal Spetrum. When $2f_s/R_c$ is odd, note the spectrum of TD-AltBOC modulated signal is $G^{\mathrm{odd}}_{\mathrm{TD-AltBOC}}(f)$, which can be expressed as 4

$$G^{\mathrm{odd}}_{\mathrm{TD-AltBOC}}(f) = \frac{2R_{\mathrm{c}}}{(\pi f)^2}\cos^2(\frac{\pi f}{R_c})\frac{\sin^2\left(\frac{\pi f}{4f_s}\right)}{\cos^2\left(\frac{\pi f}{2f_s}\right)} \tag{6}$$

When $2f_s/R_c$ is even, note the spectrum of TD-AltBOC modulated signal is $G^{\mathrm{even}}_{\mathrm{TD-AltBOC}}(f)$, which can be expressed as 4

$$G^{\mathrm{even}}_{\mathrm{TD-AltBOC}}(f) = \frac{2R_c}{(\pi f)^2}\sin^2(\frac{\pi f}{R_c})\frac{\sin^2\left(\frac{\pi f}{4f_s}\right)}{\cos^2\left(\frac{\pi f}{2f_s}\right)} \tag{7}$$

2.3 Comparison of ACE-BOC Modulated Signal Spectrum and TD-AltBOC Modulated Signal Spectrum

Figure 1 shows the power spectral density curve of ACE-BOC(15,10;3) signal and TD-AltBOC(15,10) signal. As can be seen from the graph, the power spectral density of the ACE-BOC (15,10;3) signal and the TD-AltBOC (15,10) signal is very similar, except for the following:

(1) At the fourth order harmonic (60 MHz), the power spectral density of ACE-BOC is significantly higher than that of TD-AltBOC, because the TD-AltBOC signal has constant envelope and there is no intermodulation, ACE-BOC signal introduced the intermodulation in order to ensure the envelope constant. The effect of intermodulation is as follows: at the same transmitting power P, the useful power of the received ACE-BOC signal is $P\eta$, and $\eta = 82.7\%$ is the power efficiency. However, the useful power of the received TD-AltBOC signal is P.

(2) The power spectral density of TD-AltBOC at the central frequency is slightly higher than that of ACE-BOC, while the power spectral density curve of TD-AltBOC is slightly converging to the spectrum center at the third order harmonic (45 MHz) than the ACE-BOC power spectral density curve. Because the difference is so small, the impact is completely negligible.

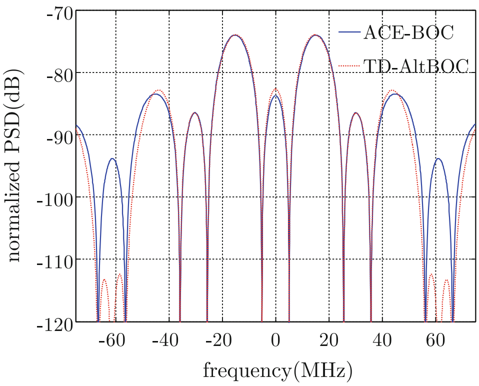

Fig. 1. The power spectral density curve of ACE-BOC and TD-AltBOC

3 Analysis Method of Navigation Performance of Satellite Navigation Signal

3.1 Pseudo-Code Tracking Accuracy

The Cremer-rao lower limit of pseudo-code tracking error is as follow [16]

$$\sigma_{\mathrm{LB}}^2 = \frac{B_{\mathrm{n}}(1 - 0.5B_nT)}{(2\pi)^2 \frac{C}{N_0} \beta_{\mathrm{rms}}^2} \tag{8}$$

Where σ_{LB}^2 represents the lower bound of the error variance of the pseudo-code tracking. B_n represents the noise bandwidth of the tracking loop. T represents the length of the integral time. C/N_0 represents the carrier-to-noise ratio. β_{rms} represents the mean square root bandwidth.

$$\beta_{\mathrm{rms}} = \int_{-B_r/2}^{B_r/2} f^2 G_{\mathrm{S},0}(f) df \tag{9}$$

Where $G_{\mathrm{S},0}(f)$ represents the normalized signal power spectral density. B_r indicates the bilateral band bandwidth of the receiver.

3.2 Anti-multipath Capability

Multipath Error Envelope. For simplicity, it is discussed that there is only one multipath signal, and the multipath error can be expressed in the following equations:

$$[R(\varepsilon - \frac{d}{2}, \gamma) - R(\varepsilon + \frac{d}{2}, \gamma)] + \alpha[R(\varepsilon - \tau - \frac{d}{2}, \gamma) - R(\varepsilon - \tau + \frac{d}{2}, \gamma)] \cos\theta \equiv 0 \tag{10}$$

In the formula, $R(\cdot,\cdot)$ represents the code correlation function, which is related to the delay and signal bandwidth. ε represents the multipath error. d represents the space between the early code and the late code of the code tracking loop discriminator. α, τ and θ represents the amplitude, delay and phase of the multipath signal relative to the direct signal respectively.

Set the multipath amplitude as α, when $\theta = 0^\circ$ and $\theta = 180^\circ$, the multipath error reaches the maximum and minimum values respectively, and the variation curve of multipath error on multipath delay, that is, multipath error envelope curve, is obtained on this condition. The maximum absolute value of the multipath error envelope indicates the worst multipath error.

The Expectation of Multipath Error Envelope. The normalized probability density function of multipath signal with different amplitude and delay can be described as follows [17]

$$p(\tau) = \frac{3e^{-\frac{3\tau}{2\tau_0}}}{2\tau_0}[1/m] \tag{11}$$

Where τ_0 represents the typical multipath delay in a multipath environment, which is related to the type of multipath environment.

Combining the probability of multipath occurrence and multipath error envelope, the multi-path envelope expectation is obtained to describe the typical multipath error by considering the fact that the close-range multipath ratio is more likely to enter the receiver than the long-range multipath signal. Typical multipath errors can be calculated in the (12) formula:

$$E\{e\} = \frac{1}{2}\int_0^\infty \frac{[\|E_{\max}(\tau)\| + \|E_{\min}(\tau)\|]}{2} p(\tau)d\tau \tag{12}$$

Where $E_{\max}(\tau)$ and $E_{\min}(\tau)$ are respectively represent the positive and negative multipath envelopes under the condition of multipath delay being τ, and $\|\cdot\|$ represents an absolute value operation.

3.3 Anti-jamming Capability

Carrier Tracking Anti-jamming Quality Factor. Its definition is [18]

$$\mathrm{Q} = \frac{1}{\sqrt{\int_{\infty}^{\infty} \mathrm{G_{JO}(f)G_{SO}(f)df}}} Q_{CR\_T} = \frac{1}{\int\limits_{-\infty}^{\infty} G_{S,0}(f)G_{I,0}(f)df} \tag{13}$$

In the formula, the normalized signal and the interference power spectral density function are represented as $G_{S,0}(f)$ and $G_{I,0}(f)$ respectively.

Pseudo-Code Tracking Anti-jamming Quality Factor. Its definition is [18]

$$Q_{CD\_T} = \frac{\int_{-\infty}^{\infty} f^2 G_{S,0}(f)df}{\int_{-\infty}^{\infty} f^2 G_{S,0}(f) G_{I,0}(f)df} \tag{14}$$

3.4 Compatibility

Spectral Separation Coefficient. Its definition is [19]

$$\chi_{S,I} = \int_{-\infty}^{\infty} G_{S,0}(f) G_{I,0}(f)df \tag{15}$$

Code Tracking Spectrum Sensitivity Coefficient. Its definition is [19]

$$\eta_{S,I} = \frac{\int_{-\infty}^{\infty} G_{S,0}(f) G_{I,0}(f) \sin^2(\pi f \Delta)df}{\int_{-\infty}^{\infty} G_{S,0}(f) \sin^2(\pi f \Delta)df} \tag{16}$$

In the formula, Δ indicates the interval between the early code correlator and the late code correlator.

4 Analysis of Navigation Performance of the ACE-BOC Modulation Signal and the TD-AltBOC Modulation Signal

The trend of the new generation GNSS receiver processing technology is to use the navigation channel to complete the measurement of the pseudo-distance and the carrier, and the data channel is only used for message demodulation. The following is for comparison of the pseudo-code tracking accuracy, multipath performance, anti-jamming performance and compatibility of the pilot channel of the two modulation signals ACE-BOC(15,10;3) and TD-AltBOC(15,10). If there is no special description below, it refers to the pilot channel signal.

4.1 Pseudo-Code Tracking Accuracy

The pseudo-code tracking accuracy of the two signals are compared under the condition of the same transmitting signal power and receiver loop parameters. Without losing generality, the total carrier-to-noise ratio of the transmitting signal is 45 dB-Hz, considering the power efficiency and the ratio power between the pilot channel and the data channel, the double-sideband received carrier-to-noise ratio of the ACE-BOC pilot signal can be calculated as 45–10 lg (87.2% × 3/4) = 43.2 (dB-Hz), and that of the TD-AltBOC pilot signal is 45–10 lg(1/2) = 42 (dB-Hz). It can be seen that under the same transmission power conditions, the carrier-to-noise ratio of the ACE-BOC pilot signal is 1.2 dB larger than the TD-AltBOC pilot signal. Set the loop noise bandwidth 0.5 Hz, the integration time 5 ms and the signal bandwidth 71.61 MHz, the pseudo-code tracking accuracy of the two signals are calculated according to formula (1) and shown in Table 1.

Table 1. Comparison of pseudo-code tracking accuracy between ACE-BOC(15,10;3) and TD-AltBOC(15,10)

Signal	CNR (dB-Hz)	Mean square root bandwidth (MHz)	Pseudo-code tracking accuracy (m)
ACE-BOC (15,10; 3)	43.2	14.29	0.016
TD-AltBOC (15,10)	42	14.20	0.019
TD-AltBOC (15,10)	43.2	14.20	0.016

As can be seen from the table, the ACE-BOC signal has a higher pseudo-code tracking accuracy than the TD-AltBOC signal for the following reasons:

(1) Under the same transmission power condition, because the pilot channel is allocated a higher power ratio the ACE-BOC(15,10;3) signal can eventually obtain a 1.2 dB higher carrier-to-noise ratio compared with the TD-AltBOC(15,10) signal, even if the power efficiency of ACE-BOC (15,10;3) is lower than that of TD-AltBOC(15,10).

(2) ACE-BOC (15,10;3) signal has a slightly larger mean square root bandwidth compared with the TD-AltBOC(15,10) signal. This is because the power spectrum of the TD-AltBOC modulation is more converging to the central frequency point (seen in Fig. 1), so its mean square root bandwidth is smaller, but the inducing difference of pseudo-code tracking accuracy is negligible. This can be seen from the Table 1 that the pseudo-code tracking accuracy of the two signals are the same under the same carrier-to-noise ratio condition.

4.2 Anti-multipath Capability

Use the coherent early-later delay lock loop, and set the early code and the later code interval 0.5 chip, the signal bandwidth 71.61 MHz. When the amplitude of the multipath signal relative to the direct TD-AltBOC pilot signal is −3 dB, because the level of ACE-BOC pilot signal is 1.2 dB higher than that of the TD-AltBOC pilot signal under the same transmission power condition, the amplitude relative to the direct ACE-BOC pilot signal is −4.2 dB. According to formula (3), the multipath envelope of the TD-AltBOC pilot signal and that of the ACE-BOC pilot signal are obtained as shown in Fig. 2(a). And similarly, when the multipath signal is 10 dB relative to the direct TD-AltBOC pilot signal, its amplitude is −11.2 dB relative to the direct ACE-BOC pilot signal, and according to the formula (3) the multipath envelope of the TD-AltBOC pilot signal and that of the ACE-BOC pilot signal are obtained as shown in Fig. 2(b).

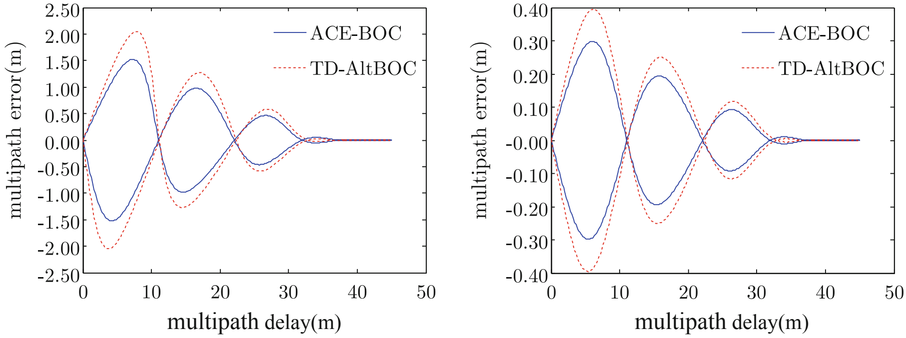

(a)The relative amplitude of the multi-path signals are -3 dB, -4.2 dB respectively

(b)The relative amplitude of the multi-path signals are -10 dB,-11.2 dB respectively

Fig. 2. The multipath Error Envelope curve of two signals TD-AltBOC(15,10) and ACE-BOC (15,10; 3)

Taking the rural or suburban environment as an example, $\tau_0 = 90$ m, in the two cases of the amplitude of the multipath signal relative to the TD-AltBOC signal respectively −3 dB and −10 dB, the multipath error of two signals are calculated according to the formula (4) and shown in Table 2.

Table 2. Comparison of multipath errors between ACE-BOC 15,10;3) and TD-AltBOC (15,10)

Conditions	Case 1		Case 2	
Signal	TD-AltBOC (15,10)	ACE-BOC (15,10;3)	TD-AltBOC (15,10)	ACE-BOC (15,10;3)
Multipath amplitude (dB)	−3	−4.2	−10	−11.2
Worst multipath error (m)	2.05	1.52	0.04	0.03
Typical multipath error (m)	0.18	0.14	0.40	0.30

It can be seen from the above table that the ACE-BOC signal has better anti-multipath capability than the TD-AltBOC signal. And its reasons are analyzed as follows:

(1) The power amplitude factor. The pilot channel power of the ACE-BOC(15,10;3) signal is 1.2 dB higher than that of the TD-AltBOC(15,10) signal, which directly leads to a better anti-multipath capability of the ACE-BOC(15,10;3) signal.

(2) The power spectrum shape factor. In order to separate the influence of power amplitude, the calculation results of −3 dB and −10 dB of multipath signal relative to direct signal show that when the power of received signal is equal, the worst multipath error of the ACE-BOC signal is mm order of magnitude lower than that of the TD-AltBOC signal, And the typical multipath error is 0.1 mm order of magnitude higher. Visibly the multipath error difference caused by the difference in the shape of the power spectrum is negligible.

4.3 Anti-jamming Capability

The anti-jamming quality factor of two signals ACE-BOC and TD-AltBOC are calculated according to the formula (6) and (7), as shown in Table 3.

Table 3. Comparison of anti-jamming quality factors between ACE-BOC(15,10;3) and TD-AltBOC(15,10)

Signal	Carrier tracking anti-jamming quality factor (dB)		Code tracking anti-jamming quality factor (dB)	
	Matched spectral interference	Single carrier interference	Matched spectral interference	Single carrier interference
ACE-BOC (15,10;3)	74.57	72.02	73.89	71.02
TD-AltBOC (15,10)	74.65	72.16	73.95	71.22

It can be seen from Table 3 that:

(1) The anti-jamming quality factor of the TD-AltBOC (15,10) is 0.1 dB–0.2 dB higher than that of the ACE-BOC(15,10;3).
(2) The maximum tolerated interference-signal-ratio is proportional to the anti-jamming quality factor, so the maximum tolerated interference-signal-ratio of the TD-AltBOC(15,10) is 0.1 dB–0.2 dB higher than that of the ACE-BOC(15,10;3).
(3) The signal level of the TD-AltBOC(15,10) is 1.2 dB lower than that of the ACE-BOC(15,10;3), therefore, its maximum tolerated interference signal level can be 1.0 dB–1.1 dB lower than that of the ACE-BOC(15,10; 3), that is, its anti-jamming ability is 1.0 dB–1.1 dB lower than that of the ACE-BOC(15,10; 3).

4.4 Compatibility

The spectral separation coefficients and the code tracking spectral sensitivity coefficients of the two signals ACE-BOC and TD-AltBOC are respectively calculated according to formula (8) and formula (9) and shown in Table 4 and Table 5. The modulation mode of the GPS L5 signal in the table is BPSK (10) with the signal bandwidth of 24 MHz; and that of the Galileo E5 signal is AltBOC (15,10) with the signal bandwidth of 51.150 MHz.

Table 4. Comparison of spectral separation coefficients between ACE-BOC(15,10;3) and TD-AltBOC(15,10)

Signal	Self spectral separation coefficient (dB)	Spectral separation coefficient to GPS L5 (dB)	Spectral separation coefficient to Galileo E5 (dB)
ACE-BOC (15,10;3)	−74.57	−85.06	−74.44
TD-AltBOC (15,10)	−74.65	−84.13	−74.49

Table 5. Comparison of code tracking spectral sensitivity coefficients between ACE-BOC (15,10;3) and TD-AltBOC(15,10)

Signal	Self-spectral sensitivity coefficient(dB)	Spectral sensitivity coefficient to GPS L5 (dB)	Spectral sensitivity coefficient to Galileo E5 (dB)
ACE-BOC (15,10;3)	−74.54	−89.98	−74.43
TD-AltBOC (15,10)	−74.51	−89.43	−74.49

It can be seen from Tables 4 and 5 that:

(1) The spectral separation coefficient of the ACE-BOC(15,10;3) is −0.9 dB–0.1 dB different to that of the TD-AltBOC(15,10).
(2) Because the signal level of the ACE-BOC(15,10;3) is 1.2 dB higher than that of the ACE-BOC(15,10), the carrier-to-noise ratio decreasing caused by its mutual interference is 1.1 dB–2.1 dB less than that of the TD-AltBOC(15,10).

5 Conclusion

The ACE-BOC and the TD-AltBOC are two kinds of four-component signal constant envelope multiplex modulation modes. In this paper, the navigation performance of the ACE-BOC(15,10;3) modulation signal and the that of the TD-AltBOC (15,10) modulation signal are compared, and its mechanisms are studied. Firstly, the power spectral density function and the power level of each channel are analyzed, then the pseudo-code tracking accuracy, anti-multipath capability, anti-jamming capability and compatibility are compared, and the mechanisms of the performance difference between the two signals are analyzed.

The results show that there is little difference between the power spectral density function curve shape of the TD-AltBOC(15,10) modulation signal and that of the ACE-BOC(15,10;3) modulation signal, and the distributed signal level of the ACE-BOC (15,10;3) pilot channel is 1.2 dB higher than that of the TD-AltBOC(15,10) pilot channel. Equivalently to the input signal level, the pseudo-code tracking accuracy and the anti-multipath capability of the ACE-BOC(15,10;3) pilot channel are 1.2 dB superior to that of the TD-AltBOC(15,10) pilot channel. The anti-jamming ability and compatibility of the ACE-BOC(15,10;3) pilot channel are respectively 1.0 dB–1.1 dB and 1.1 dB–2.1 dB superior to that of the TD-AltBOC(15,10) pilot channel. In short, the ACE-BOC(15,10;3) has a 1.0 dB–2.1 dB superior performance than the TD-AltBOC(15,10). The analysis results show that the difference of performance between the two signal is mainly caused by the power spectral density function shape difference and 1.2 dB power level distribution difference.

The research results of this paper can be used as a reference for the optimization of the satellite navigation signal modulation mode.

References

1. Zhu, X., Huang, X., Chengeng, S., et al.: Constant envelope modulation and multiplexing technologies for BDS global navigation signals. J. Nat. Univ. Defense Technol. **39**(05), 6–13 (2017)
2. Yan, T., Wang, Y., Qu, B., et al.: Constant envelope multiplexing methods for the modernized GNSS signals. Space Electron. Technol. **14**(05), 27–33, 40 (2017)
3. Cai, M., Xie, J., Wang, G.: Study of constant-envelop multiplex algorithm in satellite navigation systems. Electron. Des. Eng. **24**(07), 70–72, 75 (2016)
4. Tang, Z., Zhou, H., Wei, J., et al.: TD-AltBOC: a new COMPASS B2 modification. Sci. China Phys. Mech. Astron. **54**(6), 1014–1021 (2011)
5. Wang, Y., Meng, Y., Tao, X., et al.: Analysis of 2 order complex FIR filter effects on TD-AltBOC satellite navigation signal. Space Electron. Technol. **12**(6), 61–66 (2015)
6. Liu, K., Zhu, S., Wang, Y., et al.: Fast acquisition based on PMF-FFT for TD-AltBOC. In: China Satellite Navigation Conference (CSNC) 2015, China Satellite Navigation System Management Office Academic Exchange Center: Organizing Committee of China Satellite Navigation Conference, Xi'an, China, pp. 66–71 (2015)
7. Zhang, J., Yao, Z., Lu, M.: Applications and low-complex implementations of ACE-BOC multiplexing. In: Proceedings of the 2014 International Technical Meeting of the Institute of Navigation, pp. 781–791. The Institute of Navigation, San Diego (2014)
8. Gao, Y., Li, C., Fu, L., et al.: Overall performance comparison of three dual-frequency constant envelop modulation schemes for GNSS frequency. In: China Satellite Navigation Conference (CSNC) 2016 Proceeding: Volume II, China Satellite Navigation System Management Office Academic Exchange Center: Organizing Committee of China Satellite Navigation Conference, Changsha, China, pp. 47–56 (2016)
9. Yao, Z., Lu, M.: Constant envelope combination for components on different carrier frequencies with unequal power allocation. In: International Technical Meeting of the Institute of Navigation, pp. 629–637. The Institute of Navigation, San Diego (2013)
10. Zhang, X., Zhang, X., Yao, Z., Lu, M.: Implementations of constant envelope multiplexing based on extended interplex and inter-modulation construction method. In: Proceeding of 25th International Technical Meeting of the ION Satellite Division, pp. 893–900. The Institute of Navigation, Nashville (2012)
11. Zhu, L., Yao, Z., Lu, M., Feng, Z.: Non-symmetrical ALTBOC multiplexing for Compass B1 signal design. J. Tsinghua Univ. (Sci. Technol.) **52**(6), 869–873 (2012)
12. Guo, F., Yao, Z., Mingquan, L.: BS-ACEBOC: a generalized low-complexity frequency constant-envelop multiplexing modulation for GNSS. GPS Solutions **19**(6), 1–15 (2016)

13. Yao, Z., Zhang, J., Mingquan, L.: ACE-BOC: dual-frequency constant envelope multiplexing for satellite navigation. IEEE Trans. Aerosp. Electron. Syst. **52**(2), 1–18 (2016)
14. Yao, Z., Lu, M.: Design, implementation, and performance analysis of ACE-BOC modulation. In: Proceeding of 26th International Technical Meeting of the ION Satellite Division, pp. 361–368. The Institute of Navigation, Nashville, Tennessee (2013)
15. European Union: European GNSS (Galileo) Open Service Signal In Space Interface Control Document, Issue 1.1, pp. 5–6. European Union (2010)
16. Betz, J.W., Kolodziejski, K.R.: Generation theory of code tracking with an early-late discriminator part I: lower bound and coherent processing. IEEE Trans. Aerosp. Electron. Syst. **45**(4), 1538–1564 (2009)
17. Hein, G.W., Avila-Rodriguez, J.-A.: Combined Galileo PRS and GPS M-code. Inside GNSS **1**(1), 48–55 (2006)
18. Li, C., Chu, H., Wang, H.: Analysis of the anti-jamming performance of BOC modulated signal. J. Geomatics Sci. Technol. **29**(6), 414–417 (2012)
19. Soualle, F., Burger, T.: Introduction of an additional radio frequency compatibility criterion for code tracking performance. In: ION GNSS 20th International Technical Meeting of the Satellite Division, pp. 1201–1210. The Institute of Navigation, Forth Worth (2007)